TEMPORAL CONTROL OF RADIATION PULSE USING GAS FILLED DRIFT CELLS ON HERMES III*

T. W. L. Sanford, D. R Welch,† and R. C. Mock††
Sandia National Laboratories
P. O. Box 5800, Albuquerque, NM 87185-5800

Abstract

Significant erosion of the front of the HERMES-III electron beam in drift cells filled with N_2 gas is measured for pressures greater than 100 Torr (as much as 10 ns [3 m of beam length] at 630 Torr for 11-m length cells). Little rise time (RT) sharpening or pulse width reduction of the subsequent radiation pulse generated at bremsstrahlung targets terminating the cells, however, is measured. Three-dimensional numerical simulations show that the increased virulence of the resistive-hose instability with increased pressure degrades the spatial coherence of the leading edge of the beam, degrading in turn the RT of the radiation pulse. Transport in the lower-pressure ion-focused regime, on the other hand, does permit intense radiation fields to be produced near the beam axis at the target, with RTs and pulse widths that can be controlled with pressure. Over the range 5 to 50 mTorr, the RT and full-width half-maximum (FWHM) of the on-axis radiation pulse are inversely related to pressure and can be varied from ~5 to ~2 ns and ~8 to ~3 ns, respectively. At 10 mTorr, for example, the RT and FWHM are 4.2±1.7 ns and 6.1±1.3 ns, and the corresponding peak dose, peak-dose rate, and useful area of exposure are ~25 krad (CaF_2), ~4 Trad (CaF_2)/s, and ~300 cm^2, respectively.

Introduction

Drift cells filled with gas placed between electron-beam diodes and bremsstrahlung producing targets have been used to vary the temporal electron-beam profile and the associated bremsstrahlung pulse from pulsed gamma-ray simulators.[1] Such variations—particularly rise time and pulse width reduction—are often desired in the study of radiation effects induced by intense bursts of gamma rays.

In this paper, we explore the rise time and pulse width reduction of the bremsstrahlung pulse measured for the HERMES-III beam,[2] when the beam is injected into N_2-filled drift cells of length l (Fig. 1) varied from a few 10s of centimeters to 11 meters and when the pressure is varied over six orders-of-magnitude from 1 mTorr to atmosphere. This pressure range covers beam transport in two distinct propagation regimes (Fig. 2): the resistive-collisional regime above 200 mTorr[3] and the ion-focused regime (IFR) below 100 mTorr.[4] For these two regimes, we have developed models [5,6] that qualitatively describe the propagation characteristics of the HERMES-III beam. In the following, the radiation measurements are compared with the model expectations. The comparisons give insight into the basic mechanisms controlling the RT and FWHM of the radiation pulse. Before we quantify these characteristics, however, we briefly review the experimental arrangement.

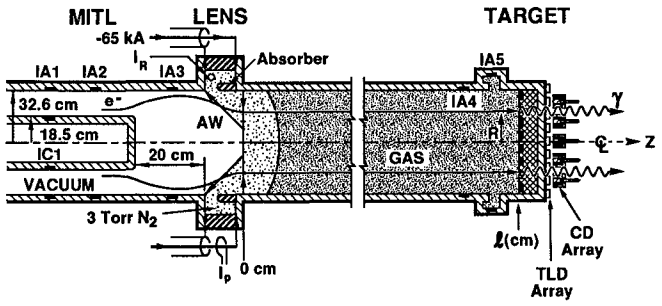

Figure 1. Schematic of the experimental arrangement showing the radial dimensions of the HERMES-III magnetically-insulated transmission line (MITL), the compound-lens diode, the gas-filled drift cell of length l, the bremsstrahlung target, and the location of the thermoluminescent dosimeter (TLD) and Compton diode (CD) radiation detectors.

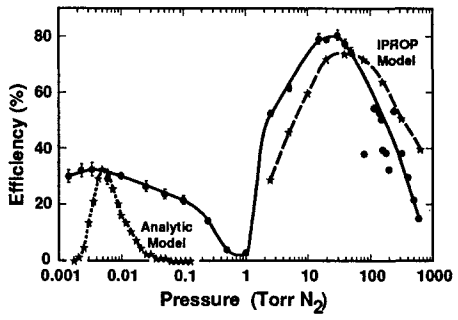

Figure 2. Energy transport efficiency measured in calorimeter target as a function of pressure, for l = 11 m. Shown also is the two-dimensional IPROP model of Ref. 5 for the collisional regime and the analytic model of Ref. 6 for the IFR. The peak efficiency of the analytic model is scaled to the peak efficiency measured in the IFR.

Experimental Arrangement

The compound-lens diode[7,8] is used to inject a 12-cm average radius annular electron beam with an average injection angle of 5.5° from the HERMES-III accelerator into a 32.6-cm radius drift cell with aluminum walls (Fig. 1). This arrangement permits beam transport in both propagation regimes. The details of the configuration are discussed in Refs. 5 and 6.

The parameters of the electron beam at the diode are identical to those summarized in Ref. 9. Essentially, the peak current and kinetic energy of the electrons injected into the drift cell are 655±14 kA and 18.3±0.5 MeV (0.7 MeV is lost in traversing the three 0.3-mm thick Ti windows of the lens and drift cell), respectively (Fig. 3). The 10-to-90% rise time (RT) and the full-width half-maximum (FWHM) of the injected current pulse are ~12 ns and 34±2 ns, respectively. The measured current growth time to peak is ~20±1.4 ns. The turn-on of this injected current corresponds to the origin of our time scale.

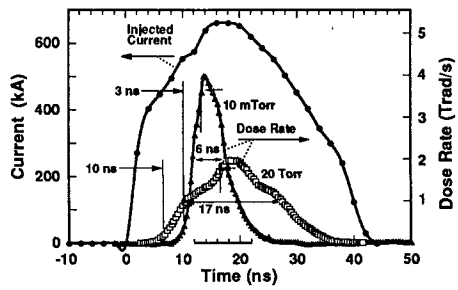

Figure 3. Comparison of the injected current pulse with the measured on-axis radiation pulse, when the pressure is 10 mTorr (shot 3039) and 20 Torr (shot 2672), the optimized Ta/C target is used, and l = 11 m. The corresponding RTs (FWHM) of the radiation pulses are 3 ns (6 ns) and 10 ns (17 ns), for shots 3039 and 2672, respectively.

Either a graphite, optimized Ta/C bremsstrahlung,[8] or graphite-calorimeter target is placed at the end of the drift cell that stops the

*This research was supported by the U. S. Department of Energy under contract DE-AC04-76DP00789.
†Mission Research Corporation, Albuquerque, NM 87106
††Ktech Corporation, Albuquerque, NM 87110

Report Documentation Page

Form Approved
OMB No. 0704-0188

1. REPORT DATE	2. REPORT TYPE	3. DATES COVERED
JUN 1993	**N/A**	**-**

4. TITLE AND SUBTITLE
Temporal Control Of Radiation Pulse Using Gas Filled Drift Cells On Hermes Ill Control

5a. CONTRACT NUMBER
5b. GRANT NUMBER
5c. PROGRAM ELEMENT NUMBER

6. AUTHOR(S)

5d. PROJECT NUMBER
5e. TASK NUMBER
5f. WORK UNIT NUMBER

7. PERFORMING ORGANIZATION NAME(S) AND ADDRESS(ES)
Sandia National Laboratories P.0. Box 5800, Albuquerque, NM 87185-5800

8. PERFORMING ORGANIZATION REPORT NUMBER

9. SPONSORING/MONITORING AGENCY NAME(S) AND ADDRESS(ES)

10. SPONSOR/MONITOR'S ACRONYM(S)
11. SPONSOR/MONITOR'S REPORT NUMBER(S)

12. DISTRIBUTION/AVAILABILITY STATEMENT
Approved for public release, distribution unlimited

13. SUPPLEMENTARY NOTES
See also ADM002371. 2013 IEEE Pulsed Power Conference, Digest of Technical Papers 1976-2013, and Abstracts of the 2013 IEEE International Conference on Plasma Science. Held in San Francisco, CA on 16-21 June 2013. U.S. Government or Federal Purpose Rights License.

14. ABSTRACT
Significant erosion of the front of the HERMES-III electron beam in drift cells filled with N2 gas is measured for pressures greater than 100 Torr (as much as 10 ns [3m of beam length] at 630 Torr for 11-m length cells). Little rise time (RT) sharpening or pulse width reduction of the subsequent radiation pulse generated at bremsstrahlung targets terminating the cells, however, is measured. Three-dimensional numerical simulations show that the increased virulence of the resistivehose instability with increased pressure degrades the spatial coherence of the leading edge of the beam, degrading in turn the RT of the radiation pulse. Transport in the lower-pressure ion-focused regime, on the other hand, does permit intense radiation fields to be produced near the beam axis at the target, with RTs and pulse widths that can be controlled with pressure. Over the range 5 to 50 mTorr, the RT and full-width halfmaximum (FWHM) of the on-axis radiation pulse are inversely related to pressure and can be varied from -5 to -2 ns and -8 to -3 ns, respectively. At 10mTorr,forexample, theRTandFWHMare4.2±1.7 ns and 6.1±1. 3 ns, and the corresponding peak dose, peak -dose rate, and useful area of exposure are -25 krad (CaF2), -4 Trad (CaF2)/s, and -300 cm2, respectively.

15. SUBJECT TERMS

16. SECURITY CLASSIFICATION OF:			17. LIMITATION OF ABSTRACT	18. NUMBER OF PAGES	19a. NAME OF RESPONSIBLE PERSON
a. REPORT	b. ABSTRACT	c. THIS PAGE			
unclassified	**unclassified**	**unclassified**	**SAR**	**4**	

primary beam electrons. The resulting measured radiation, unless otherwise specified, is scaled to that of the graphite target. On the downstream face of the targets, a 48-element array of thermoluminescent dosimeters (TLDs) is placed, which enables the radial radiation-dose profile to be determined. Immediately downstream of the array, a set of five Pb collimated Compton diodes (CDs)[10] are centered along the x-axis at 0, ±13, and ±26 cm. These monitors are sensitive to the temporal as well as the coupled spatial characteristics of the incident radiation.

We now quantify the characteristics of the radiation measured in these diagnostics, first in the collisional regime and then in the ion-focused regime. The emphasis of the measurements is on the variation in RT, FWHM, and magnitude of the radiation that is achievable as a function of gas pressure.

Resitive-Collisional Regime

In the resistive-collisional regime, the beam is rapidly charge neutralized and nearly current neutralized. The transverse motion of the beam is contained by the azimuthal self-magnetic field resulting from the residual net current (beam current plus the electron-plasma return current). The variation in the average peak dose rate measured in the Compton diodes with pressure (Fig. 4) roughly tracks the variation in the energy transport efficiency with pressure measured in the calorimeter target (Fig. 2). Maximum energy transport and corresponding radiation output in the collisional regime occurs at ~20 Torr (Figs. 2 and 4). The 20-Torr optimum is a trade-off between improved magnetic confinement versus increased inductive, beam-front erosion, and collisional losses as the pressure is increased. For reference, the corresponding radial dose profile measured in the TLD array and the associated on-axis radiation pulse is given in Figs. 5 and 3, respectively, when the drift-cell length is 11 m and the optimized Ta/C target is used. Under these conditions at 20 Torr the peak dose, the useful exposure area (area enclosed by the radius where the dose is greater than half the peak dose), the peak-dose rate, the average RT, and average FWHM of the radiation pulse at the downstream face of the target are 34 krad, 2300 cm^2, 2 Trad/s, 11±2.2 ns, and 14.3±2.6 ns, respectively. "Average" refers to the mean of the specified quantity measured in the five Compton diodes. The uncertainties refer to rms shot-to-shot variation.

Above 100 Torr, significant erosion of the beam front occurs in agreement with our two-dimensional (2D) IPROP[11] simulations[5] (Fig. 6). The erosion is due to charge neutralization processes, which extract energy from the front of the beam. At 630 Torr, erosion removes about 10 ns (3 m of length) from the beam front when l = 11 m. For shorter l the erosion is less, as expected.

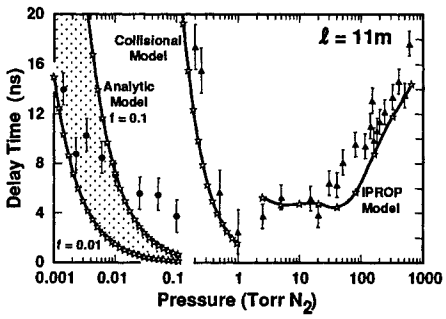

Figure 6. Comparison of the turn-on time of the radiation pulse as a function of pressure for l = 11 m. Shown are the predictions of the 2D-IPROP model[5] for the high-pressure collisional regime, the analytic collisional model[6] for the low-pressure collisional regime, and the analytic IFR-model bounds[6] (f = 0.01 and f = 0.1) for the IFR regime. The data in the collisional regime (▲) corresponds to the average of the five CD detectors. The data in the IFR (●) corresponds to that taken on axis.

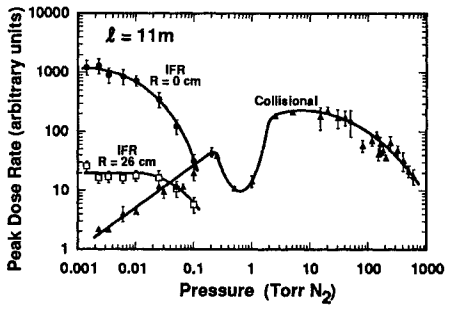

Figure 4. Relative peak dose rates measured in the CDs as a function of pressure for l = 11 m. The data in the collisional regime (▲) corresponds to the average of the five CD detectors. The data in the IFR corresponds to that measured on axis (R = 0 cm [●]) and off axis at R = 26 cm (□).

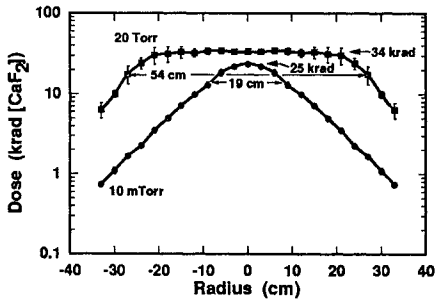

Figure 5. Comparison of the radial radiation dose profiles measured in the TLD array, when the pressure is 10 mTorr and 20 Torr; the optimized Ta/C target is used, and l = 11 m. At 10 mTorr and 20 Torr, the corresponding dose-area products measured at the downstream target face are 16 and 80 Mrad (CaF_2)· cm^2, respectively. Figure 3 shows the associated on-axis radiation pulses.

Intuitively, the erosion is expected to reduce the RT and FWHM of the beam-pulse incident at the target and the associated radiation pulse. In agreement with intuition, our 2D IPROP model shows that the RT and FWHM of the radiation pulse are reduced when the pressure is increased. When l = 11 m, the model shows that the RT should be reduced by a factor of two (Fig. 7) and that the FWHM should show a slight reduction (Fig. 8) over the above pressure range. The average radiation measurements at l = 2.5, 4.35, and 11 m (Figs. 7 and 8), however, indicate little systematic pulse sharpening or pulse-width reduction with pressure. The rms variation in either the RT or the FWHM among the five Compton-diode signals used in the average is typically 3 ns for pressures greater than 1 Torr. The uncertainties shown in Figs. 7 and 8 are the associated statistical error in the measured average.

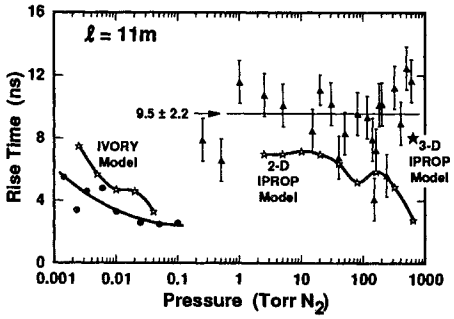

Figure 7. Comparison of the rise time of the radiation pulse as a function of pressure for l = 11 m. Shown are the predictions of the 2D- and 3D-IPROP model[5] for the high-pressure collisional regime, and the IVORY model[14] for the low-pressure IFR regime. The data in the collisional regime (▲) corresponds to the average of the five CD detectors. The data in the IFR (●) corresponds to that taken on axis.

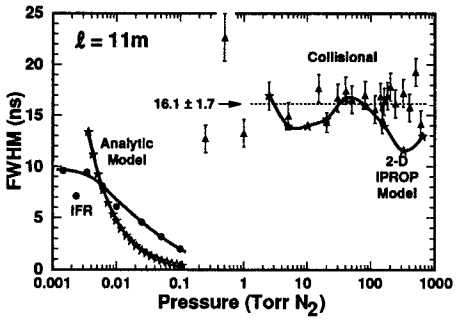

Figure 8. Comparison of the full-width half-maximum (FWHM) of the radiation pulse as a function of pressure for l = 11 m. Shown are the predictions of the 2D-IPROP model[5] in the collisional regime and the IFR analytic model[6] (where FWHM is proportional to the time between when f = 0.1 and f = 1 is reached) in the IFR. The data in the collisional regime (▲) corresponds to the average of the five CD detectors. The data in the IFR (●) corresponds to that taken on axis.

This lack of observed RT sharpening (expected from the erosion of the beam front with increasing pressure) is likely due to the simultaneous increase in the effects of the resistive hose instability. Three-dimensional (3D) IPROP simulations show that this instability produces radial oscillations in the centroid of the beam,[5,12] resulting in the beam scraping the wall of the drift cell and degrading the leading edge of the beam at the target and the subsequent radiation pulse. Figure 9, for example, contrasts the 2D and 3D simulation of the beam charge lost to the wall and the associated radiation pulse, when a 1.5 cm high-frequency off-set is given the beam in the 3D simulation at injection, for l = 11 m and a pressure of 640 Torr. Such an injection off-set is typically measured and, in the simulation, leads to a 10-cm off-set at the target. Figure 9 shows that this off-set produces significant losses for both short as well as long distances along the wall of the drift cell, perhaps explaining why little pulse sharpening (aside from the decreased erosion) is observed at the shorter lengths measured. Moreover, the simulations show that the 2.8-ns RT generated in 2D increases to 8.1 ns in the 3D simulation (Fig. 7). This 3D simulation is consistent with the 9.3±2.2 ns measured.

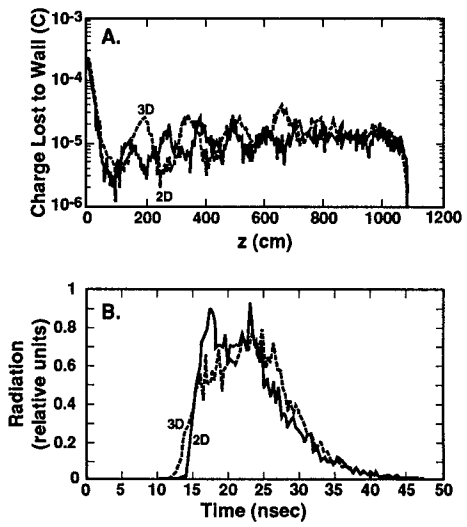

Figure 9. Comparison between the 2D- and 3D-IPROP model simulations of (A) charge lost to the wall of the drift cell, and (B) the shape of the average radiation pulse generated at the target, for l = 11 m and a pressure of 640 Torr.

Below 1 Torr beam transport is limited in the collisional regime early in the beam pulse by strong beam-plasma instabilities such as two-stream and hollowing.[5,6] Two-stream delays collisional transport until late in the beam pulse, when the instabilities are sufficiently damped by the low-energy plasma electrons created by the continued beam-gas ionization process (Fig. 6). As the pressure is reduced the two-stream is damped progressively later, leading to reduced energy transport in the collisional regime (Fig. 4). The hollowing instability initially disrupts collisional beam transport until net currents are minimized near 1 Torr.

As the pressure decreases below 100 mTorr, however, an additional transport mode (IFR) becomes available early in the beam pulse. In this regime the beam space charge ejects just plasma electrons, leaving enough positive plasma ions to electrostatically contain the transverse motion of the beam. The radiation observed in this regime has the useful characteristics that we were attempting to achieve in the collisional regime by beam erosion, namely RT sharpening and pulse width reduction, as we now show.

Ion-Focused Regime

In the IFR the beam does not propagate more than a few meters until the charge neutralization fraction f (defined as the ratio of the plasma ion to beam charge density), resulting from the beam impact ionization and subsequent plasma-electron and plasma-ion avalanche, grows sufficiently to allow the beam to overcome the space-charge depression at injection. For the HERMES-III beam this value lies roughly between 0.01 and 0.1. Propagation beyond injection occurs only when f > 0.01 such that the beam dispersion is contained by the potential of the plasma ions. f continues to increase near injection from the continued ionization processes, eventually exceeding unity. The space charge of the beam is then globally neutralized, and the newly ionized plasma electrons are no longer expelled. The plasma electrons remaining interact with the beam, forming a two-stream instability that rapidly terminates propagation. Because f increases with increasing pressure, the time delay before propagation occurs (i.e., when f ~ 0.01 to 0.1 as shown in Fig. 6) and the width of the subsequent propagation pulse (Fig. 8) decrease with increasing pressure. The measured time delay and width of the on-axis radiation pulse exhibit these trends and are in qualitative agreement with this analytic model[6] (Figs. 6 and 8). Increasing the pressure from 1.4 mTorr to 100 mTorr reduces the FWHM of the radiation pulse measured on-axis from ~10 to ~2 ns.

The final phase of the IFR propagation involves the contraction of the beam at the target. The conducting target shorts out the self-repulsive radial electric fields while leaving the attractive self-magnetic force unaffected. The beam thus receives a sudden inward impulse, causing the beam to radially sweep in at the target. The time-integrated (Fig. 5) and time-dependent (Fig. 10A) radial profiles of the radiation measured at the target show a corresponding strong enhancement about the beam axis in contrast to propagation in the collisional regime. In the collisional regime, the profile is governed by the magnetic confinement, which produces a relatively flat distribution with radius (Fig. 5 and 10B).

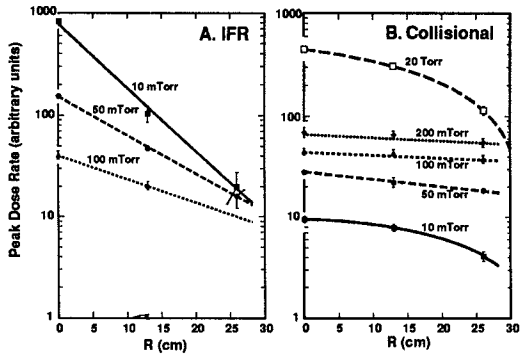

Figure 10. Comparison of the measured radial profile of the peak dose rate for the (A) IFR pulse (i.e., early pulse) and (B) the collisional pulse (i.e., later pulse) for a few descrete pressures where l = 4.4 m.

The beam contraction with time in the IFR is observed from the turn-on of the radiation measured at the target. The off-axis radiation

always occurs earlier than that measured closer to the axis. Measurements of this delay in the Compton diodes show that at 10 mTorr the radial sweep of the beam towards the axis is 5 cm/ns at the target and is in good agreement with IVORY[13] particle-in-cell simulation estimates.[14]

The fast rise time of the measured on-axis radiation is due to the combination of this radial sweeping and the delay in generating sufficient ionization for propagation to occur. It is in qualitative agreement with that modeled (Fig. 7). Measurements show that by increasing the pressure from 1.4 mTorr to 100 mTorr, the RT is reduced from >6 ns to <2 ns. The off-axis RT degrades, as expected (Table I). At large radii, the RTs and FWHMs are similar to those measured at 20 Torr.

Table I: Comparison of RT and FWHM measured in ns at 20 Torr and 10 mTorr in the Compton diodes as a function of radius, over the range $1 \le l \le 11$ m. The measured RT and FWHM of the current pulse at the diode is 11.8±1.5 ns and 33.5 ns, respectively. The graphite target was used.

	Pressure	R=0 cm	R = 13 cm	R = 26 cm
RT	20 Torr	11.4±2.2	11.5±2.0	9.0±1.9
	10 mTorr	4.2±1.7	6.9±2.4	11.7±4.9
FWHM	20 Torr	14.1±2.8	17.2±2.1	17.3±2.0
	10 mTorr	6.1±1.3	11.9±2.6	20.0±5.8

As the pressure increases above 5 mTorr, transport in the IFR early in the beam pulse begins to decline as the propagation window ($0.1 < f < 1$) shrinks (Fig. 8). Simultaneously, propagation in the collisional regime begins to accrue at the rear of the beam pulse, as the two-stream instabilities (which terminate IFR transport) are quenched by gas collisions earlier, permitting propagation in the collisional regime. The region between 5 mTorr and 100 mTorr represents a transition region between dominant IFR and collisional transport where transport in both regimes occurs (Fig. 4). Below 5 mTorr, the HERMES-III beam has insufficient length to reach the collisional regime and only the first IFR pulse is observed. Above 200 mTorr the gas breaks down too rapidly to observe a significant IFR pulse, and only the second collisional pulse is observed.

Operation from 5 mTorr to 50 mTorr provides a pressure range where significant near-axis radiation is produced whose RT and FWHM can be varied from ~5 to ~2 ns and ~8 ns to ~3 ns, respectively, without significant contamination from the late arriving collisional pulse. At 10 mTorr for example, the peak dose, the useful area of irradiation, the peak dose rate, the on-axis RT and FWHM are 25 krad, 300 cm^2, 4 Trad/s, 4.2±1.7 ns, and 6.1±1.3 ns, respectively, when the Ta/C target is used (Figs. 3 and 5). Extrapolating the dose rate measured with the graphite targets (Fig. 4) and using these measurements made at 10 mTorr with the optimized Ta/C target (Fig. 5) as a normalization, the estimated peak dose rate over the corresponding 5 to 50 mTorr range for the optimized target should vary from 5 Trad/s to 0.7 Trad/s.

Lastly, measurements taken at 10 mTorr for lengths varying from a few 10's of centimeters to 11 m show that the above characteristics are fully developed after about 4 m of drift.[6]

Summary

Collisional propagation within drift cells filled with N_2 gas enables the HERMES-III beam to be efficiently transported to bremsstrahlung targets located at the end of the cell, where radiation is produced. Despite the significant beam-front erosion that occurs at the high gas pressures studied, little reduction in RT or width of the subsequent radiation pulse in this transport regime is measured. This lack of RT sharpening is due to the increase in the virulence of the resistive-hose instability, which degrades the spatial coherence of the leading edge of the beam. At low pressure, however, transport in the ion-focused regime permits the RT and pulse width of the radiation generated at the target to be varied. In this regime, intense radiation fields are produced near the beam axis.

Acknowledgments

We thank P. W. Spence (Pulse Sciences Inc.) for useful discussions; D. Muirhead for engineering support; P. J. Skogmo, R. L. Klingler, V. Harper-Slaboszewicz, R. L. Westfall, and the HERMES-III crew for technical support; J. E. Maenchen, J. J. Ramirez, W. Beezhold, and J. E. Powell for programmatic support; and J. E. Maenchen and P. S. Raglin for reviewing and L. O. Peterson for typing this manuscript.

References

[1] M. Bushell, S. Graybill, M. Litz, and G. Merkel, *IEEE Trans. Nucl. Sci.*, **NS-31**, 1299 (1984).

[2] J. J. Ramirez, K. R. Prestwich, D. L. Johnson, J. P. Corley, G. J. Denison, J. A. Alexander, T. L. Franklin, P. J. Pankuch, T. W. L. Sanford, T. J. Sheridan, L. L. Torrison, and G. A. Zawadzkas, *Digest of Technical Papers, 7th IEEE Pulsed Power Conference* (Monterey, CA, June 11-14, 1989), pp. 26-31.

[3] M. Lampe, Navel Research Laboratory Report 6159 (March 4, 1988).

[4] H. L. Buchanan, *Phys. Fluids* **30**, 221 (1987).

[5] T. W. L. Sanford, D. R. Welch, and R. C. Mock, "Dynamics of a 19-MeV, 700-kA, 25-ns Electron Beam in a Long Collisional Gas Cell," submitted to *Phys. Fluids B* (1993).

[6] T. W. L. Sanford, D. R. Welch, and R. C. Mock, "Very High-Current Propagation in the Ion-Focused to Collision-Dominated Regime," submitted to *Phys. Fluids B* (1993).

[7] T. W. L. Sanford, J. A. Halbleib, J. W. Poukey, T. Sheridan, D. Muirhead, C. E. Yagow, K. A. Mikkelson, R. Mock, P. W. Spence, V. L. Bailey, and H. Kishi, *Digest of Technical Papers, 7th IEEE Pulsed Power Conference* (Monterey, CA, June 11-14, 1989), pp. 441-444.

[8] T. W. L. Sanford and R. C. Mock, *IEEE Trans. Nucl. Sci.*, **39**, 2060 (1992).

[9] T. W. L. Sanford, J. A. Halbleib, L. J. Lorence, J. G. Kelly, P. J. Griffin, J. W. Poukey, R. C. Mock, W. H. McAtee, and K. A. Mikkelson, *Rev. Sci. Instrum.* **63**, 4795 (1992).

[10] G. A. Carlson, T. W. L. Sanford, and B. A. Davis, *Rev. Sci. Instrum.* **61**, 3447 (1990).

[11] B. B. Godfrey and D. R. Welch, *Twelfth Conference on Numerical Simulations of Plasmas* (Lawrence Livermore National Laboratory, San Francisco, CA, 1987) Paper No. CM1.

[12] D. R. Welch, C. L. Olson, and T. W. L. Sanford, "Simulation of Charged-Particle Beam Transport in a Gas Using a Hybrid Particle-Fluid Plasma Model," submitted to *Phys. Fluids B* (1993).

[13] M. M. Campbell, B. B. Godfrey, and D. J. Sullivan, *IVORY User's Manual*, Mission Research Corp., AMRC-R-454 (1988).

[14] D. R. Welch and T. W L. Sanford, "Low Pressure Intense Relativistic Erection Beam Transport," submitted to *Phys. Fluids B* (1993).